J|A|C|S
ARTICLES
Published on Web 02/27/2007

Relationship Among Ligand Conformations in Solution, in the Solid State, and at the Hsp90 Binding Site: Geldanamycin and Radicicol

Pahk Thepchatri,[†] Tomasso Eliseo,[‡] Daniel O. Cicero,[‡] David Myles,[§] and James P. Snyder*,[†]

Contribution from the Department of Chemistry, Emory University, Atlanta, Georgia 30322, NMR Laboratory, Faculty of Chemical Sciences and Technologies, University of Rome "Tor Vergata", Rome, Italy, and Kosan Biosciences, Inc., 3832 Bay Center Place, Hayward, California 94545

Received July 8, 2006; E-mail: jsnyder@emory.edu

Abstract: The unknown effects of a receptor's environment on a ligand's conformation presents a difficult challenge in predicting feasible bioactive conformations, particularly if the receptor is ill-defined. The primary hypothesis of this work is that a structure's conformational ensemble in solution presents viable candidates for protein binding. The experimental solution profile can be achieved with the NAMFIS (NMR analysis of molecular flexibility in solution) method, which deconvolutes the average NMR spectrum of small flexible molecules into individual contributing conformations with varying populations. Geldanamycin and radicicol are structurally different macrocycles determined by X-ray crystallography to bind to a common site on the cellular chaperone heat shock protein 90 (Hsp90). Without benefit of a receptor structure, NAMFIS has identified the bioactive conformers of geldanamycin and radicicol in $CDCl_3$ solution with populations of 4% and 21%, respectively. Conversely, docking the set of NAMFIS conformers into the unliganded proteins with GLIDE followed by MM-GBSA scoring reproduces the experimental crystallographic binding poses.

Introduction

The experimental structures of highly flexible small molecules are known largely from X-ray crystallography as a result of being immobilized in a single-crystal lattice or cocrystalized in a macromolecular binding site.[1−2] NMR spectroscopy is likewise a valuable source of structural information when either a compound's conformation is rigid or its equilibrium partners can be separately determined at an appropriate low temperature or captured in the solid state. For molecules with multiple single bonds that experience rapid exchange among torsional forms on the NMR time scale, deconvolution procedures are necessary to identify and quantitate the collection of minimum energy conformations in solvents.[3−11]

Unfortunately, few studies correlate small molecule structures found in all three states: within a crystalline matrix, at a protein-binding site, and in solution. Given that each involves empirical energy minima, while the latter enjoys a multiplicity of torsional isomers, one can ask whether the immobilized forms are among the solution conformer populations. If they are, then there is a high probability that deconvolution of the averaged NMR spectrum of a macromolecular modulator can reveal the protein-bound bioactive form. Of course, subsequent analysis is necessary to distinguish the latter within the pool of 5−20 solution conformations. This is a much simpler task than extracting the same structure from, for example, several thousand fully optimized conformations generated by a complete conformational search. The process is further complicated by the prospect that computed relative energies for the latter dataset are most likely suspect.[12]

The NAMFIS (NMR analysis of molecular flexibility in solution) deconvolution method has been employed to analyze the solution structures of paclitaxel,[13] several epothilones,[14]

[†] Emory University.
[‡] University of Rome "Tor Vergata".
[§] Kosan Biosciences, Inc.

(1) (a) Bruno, I. J.; Cole, C.; Edging, P. R.; Kessler, M.; Macrae, C. F.; McCabe, P.; Pearson, J.; Taylor, R. *Acta. Crystallogr.* **2002**, *B58*, 289−397. (b) http://www.ccdc.cam.ac.uk/.
(2) (a) Berman, H. M.; Westbrook, J.; Feng, Z.; Gillard, G.; Bhat, T. N.; Weissig, H.; Shindyalov, I. N.; Bourne, P. E. *Nucleic Acids Res.* **2000**, *28*, 235−242. (b) http://pdbbeta.rcsb.org/pdb/Welcome.do.
(3) Cicero, D.; Barbato, G.; Bazzo, R. *J. Am. Chem. Soc.* **1995**, *117*, 1027−1033.
(4) Landis, C.; Allured, V. S. *J. Am. Chem. Soc.* **1991**, *113*, 9493−9499.
(5) Landis, C.; Luck, L. L.; Wright, J. M. *J. Magn. Reson., Ser. B* **1995**, *109*, 44−59.
(6) Landis, C. R.; Ros, M. A. M. P.; Horton, A. D. *Organometallics* **1998**, *17*, 5031−5040.
(7) Nikiforovich, G. V.; Vesterman, B. G.; Betins, J. *J. Biophys. Chem.* **1988**, *31*, 101−106.
(8) Nikiforovich, G. V.; Kover, K. E.; Kolodziej, S. A.; Nock, B.; George, C.; Deschamps, J. R.; Flippen-Anderson, J. L.; Marshall, G. R. *J. Am. Chem. Soc.* **1996**, *118*, 959−969.
(9) Nikiforovich, G. V.; Kover, K. E.; Zhang, W.-J.; Marshall, G. R. *J. Am. Chem. Soc.* **2000**, *122*, 3262−3273.
(10) Mierke, d. F.; Kurz, M. I.; Kessler, J. *J. Am. Chem. Soc.* **1994**, *116*, 1042−1049.
(11) Cuniasse, P.; Raynal, I.; Yiotakis, A. *J. Am. Chem. Soc.* **1997**, *119*, 5239−5248.
(12) (a) Lakdawala, A; Wang, M.; Nevins, N.; Liotta, D.C.; Rusinska-Roszak, D.; Lozynski, M.C.; Snyder, J.P. *BMC Chem. Biol.* **2001**, *1*, 2. (b) http://www.biomedcentral.com/1472-6769./1/2.
(13) Snyder, J. P.; Nevins, N.; Cicero, D. O.; Jansen, J. *J. Am. Chem. Soc.* **2000**, *122*, 724−725.

discodermolide,[15] and laulimalide.[16] For the first two molecules we hypothesized that the solution ensemble of conformers contains the bioactive form. The purpose of the work was to utilize the derived solution conformers as docking candidates for molecules that target the taxoid site of the α,β-tubulin dimer, a protein solved at 3.7 Å resolution by electron crystallography.[17] This resolution is insufficient to define either the ligand conformation or the binding mode with certainty. However, by combining a dataset of high-resolution NMR conformers and the crystallographic density from a low-resolution electron crystallographic structure, in principle the structure of a reasonable protein−ligand complex can be achieved with the help of molecular modeling. The trio of techniques has been productively integrated to develop atomic resolution tubulin−paclitaxel[18] and tubulin−epothilone models[14] from low-population (4−20%) ligand conformations, torsional isomers that cannot be observed in a rapidly equilibrating system by conventional NMR analysis. The paclitaxel−tubulin model has been substantiated by a number of subsequent studies,[19] while the epothilone model is still under evaluation.

While it appears that assuming the bioactive form to be among the solution conformations for paclitaxel and the epothilones was justified, we sought to test the hypothesis in a system where both solid-state and protein-bound conformations have been unambiguously determined. The natural antibiotic metabolites geldanamycin (**1**) and radicicol (**2**) were selected to evaluate

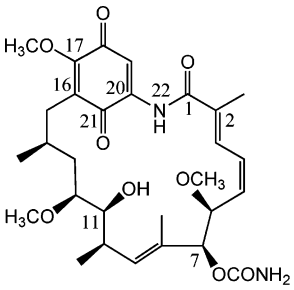

1

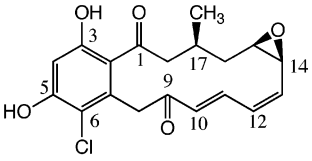

2

the concept. The compounds and various analogues have been investigated for their antitumor properties.[20] Both compounds block the growth of tumor cells by coupling with the N-terminal domain of the 90 kDa heat shock protein (Hsp90), a cellular chaperone essential to the refolding of misfolded proteins such as the oncogenic kinases HER-2, Raf-1, and AKT.[21] Hsp90 is theorized to accomplish this task by partitioning between two conformations, one active and one inactive. The former refolding-competent active form is stabilized by ATP.[22] Geldanamycin, radicicol and analogues interfere with the action of Hsp90 by efficiently competing with bound ATP and thereby promote the degradation of protooncogenic client kinases.[22] Renewed interest in the protein has led to several recent reports describing novobiocin-based blockers[23] and structurally simpler pyrazole[24] and purine[25] inhibitors.

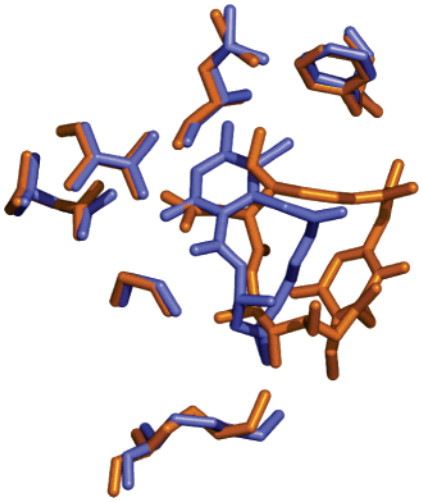

Figure 1. Geldanamycin (orange) and radicicol (blue) bound in Hsp90 crystal structures. PDB codes: 1A4H and 1BGQ, respectively. No significant changes in protein side chain conformations occur upon binding.

The X-ray crystal structures of **1** and **2** and structurally similar derivatives in complex with the N-terminal domain of Hsp90 are available at 1.8 and 2.5 Å resolution, respectively.[26−27] Although the structures of the two molecules are quite different, they bind to the same Hsp90 protein cavity, radicicol exhibiting 50−100-fold higher binding affinity (Figure 1).[27] In addition, the solid-state X-ray crystal structure of each compound has been solved in the absence of protein.[28,29] Figure 2 compares X-ray crystal structures of protein-bound *cis*-**1** and the free ligand *trans*-**1**. It is noteworthy that cyclosporin A reverses this observation; the 9,10-peptide bond is *trans* when bound to cyclophilin[30] and *cis* when uncomplexed either in $CHCl_3$ solution[31] or in the solid state.[32] This wealth of structural

(14) Nettles, J. H.; Li. H.; Cornett. B.; Krahn, J. M.; Snyder, J. P.; Downing, K. H. *Science* **2004**, *305*, 866−869.
(15) Monteagudo, E.; Cicero, D. O.; Cornett, B.; Myles, D.; Snyder, J. P. *J. Am. Chem. Soc.* **2001**, *123*, 6919−6930.
(16) Thepchatri. P.; Cicero, D. O.; Monteagudo, E.; Ghosh, A. K.; Cornett, B.; Weeks, E. R.; Snyder, J. P. *J. Am. Chem. Soc.* **2005**, *127*, 12838−12846.
(17) Nogales, E.; Wolf, S. G; Downing, K. H. *Nature* **1998**, *391*, 199−203.
(18) Snyder, J. P.; Nettles, J. H.; Cornett, B.; Downing, K. H.; Nogales, E. *Proc. Natl. Acad. Sci. U.S.A.* **2001**, *98*, 5312−5316.
(19) (a) Ganesh, T.; Yang, C.; Norris, A.; Glass, T.; Bane, S.; Ravindra, R.; Banerjee, A.; Metaferia, B.; Thomas, S. L.; Giannakakou, P.; Alcaraz, A. A.; Lakdawala, A. S.; Snyder, J. P.; Kingston, D. G. I. *J. Med. Chem.* **2007**, *50*, 713−725. (b) Paik, Y.; Yang, C.; Metaferia, B.; Tang, S.; Bane, S.; Ravindra, R.; Shanker, N.; Alcaraz, A. A.; Johnson, S. A.; Schaefer, J.; O'Connor, R. D.; Cegelski, L.; Snyder, J. P.; Kingston, D. G. I. *J. Am. Chem. Soc.* **2007**, *129*, 361−370. (c) Johnson, S. A.; Alcaraz, A.; Snyder, J. P. *Org. Lett.* **2005**, *7*, 5549−5552. (d) Liu, C.; Tamm, M.; Nötzel, M. W.; Meijere, A.; Schilling, J. K.; Lakdawala, A.; Snyder, J. P.; Bane, S. L.; Shanker, N.; Ravindra, R.; Kingston, D. G. I. *Eur. J. Org. Chem.* **2005**, 3962−3972. (e) Kingston, D. G. I.; Bane, S.; Snyder, J. P. *Cell Cycle* **2005**, *4* (2), 279−289. (f) Ganesh, T.; Guza, R. C.; Bane, S.; Ravindra, R.; Shanker, N.; Lakdawala, A. S.; Snyder, J. P.; Kingston, D. G. I. *Proc. Nat. Acad. Sci. U.S.A.* **2004**, *101*, 10006−10011. (g) Querolle, O.; Dubois, J.; Thoret, S.; Roussi, F.; Guéritte, F.; Guénard, D. *J. Med. Chem.* **2004**, *47*, 5937−5944.
(20) Rastelli, G.; Tian, Z.-Q.; Wang, Z.; Myles, D.; Liu, Y. *Bioorg. Med. Chem. Lett.* **2005**, *15*, 5016−5021.
(21) Grenert, J. P.; Sullivan, W. P.; Faddens, P.; Haystead, T. A. J.; Clark, J.; Mimnaugh, E.; Krutzsch, H.; Ochel, H.; Schulte, T. W.; Sausville, E.; Neckers, L. M.; Toft, D. O. *J. Biol. Chem.* **1997**, *272*, 23843−23850.
(22) Terry, J.; Lubieniecka, M.; Kwan, W.; Liu, S.; Nielsen, T. O. *Clin. Cancer Res.* **2005**, *11*, 5631−5638.
(23) Yu, X. M.; Shen, G.; Neckers, L.; Blake, H.; Holzbeierlein, J.; Cronk, B.; Blagg, B. S. J. *J. Am. Chem. Soc.* **2005**, *127*, 12778−12779.
(24) (a) Kreusch, A.; Han, S.; Brinker, A.; Zhou, V.; Choi, H.-S.; He, Y.; Lesley, S. A.; Caldwell, J.; Gu, X.-J. *Bioorg. Med. Chem. Lett.* **2005**, *15*, 1475−1478. (b) Cheung, K.-M. J.; Matthews, T. P.; James, K.; Rowlands, M. G.; Boxall, K. J.; Sharp, S. Y.; Maloney, A.; Roe, S. M.; Prodromou, C.; Pearl, L. H.; Aherne, g. W.; McDonald, E.; Workman, P. *Bioorg. Med. Chem. Lett.* **2005**, 15, 3338−3343. (c) Brough, P. A.; Barril, X.; Beswick, M.; Dymock, B. W.; Drysdale, M. J.; Wright, L.; Grant, K.; Massey, A.; Surgenor, A.; Workman, P. *Bioorg. Med. Chem. Lett.* **2005**, *15*, 5197−5201.
(25) Wright, L.; et al. *Chem. Biol.* **2004**, *11*, 775−785.
(26) Roe, S.; Prodromou, C.; O'Brien, R.; Ladbury, J. E.; Piper, P. W.; Pearl, L. H. *J. Med. Chem.* **1999**, *42*, 260−266.
(27) Jez, J. M.; Chen, J. C.-H.; Rastelli, G.; Stroud, R. M.; Santi, D. V. *Chem. Biol.* **2003**, *10*, 361−368.
(28) Schnur, R. C.; Corman, M. L. *J. Org. Chem.* **1994**, *59*, 2581−2584.
(29) Cutler, H. G.; Arrendale, R. F.; Springer, J. P.; Cole, P. D.; Roberts, R. G.; Hanlin, R. T. *Agric. Biol. Chem.* **1987**, *51*, 3331−3338.

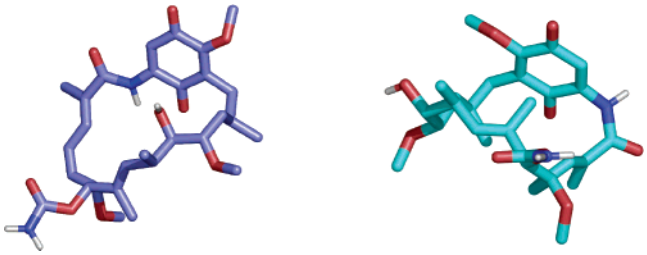

Figure 2. Solid-state (blue, *trans*-amide) and protein-bound (cyan, *cis*-amide) conformations of geldanamycin.

information triggered our interest for its value in addressing the accuracy of solution conformations as determined by NMR spectroscopy and the use of such conformations for solving the structure of certain ligand−protein complexes.

In the present work we show that, in spite of the fact that **1** and **2** incorporate 14 and 9 easily rotatable bonds within the heavy atom periphery of the corresponding flexible 19- and 14-membered rings, respectively, both solid-state and protein-bound conformations are found among the limited number of NAMFIS-derived solution conformations. We also demonstrate that docking protocols such as Schrödinger's GLIDE program[33] used in conjunction with a superior scoring function can reproduce the experimental protein−ligand complexes using the NMR-determined conformations.

Materials and Methods

Geldanamycin NMR Data. Following methods described previously,[16] geldanamycin was assigned by a combination of two-dimensional (2D) ^{1}H and ^{1}H−^{13}C experiments acquired on a Bruker Avance spectrometer operating at 400 MHz and equipped with a *z*-shielded gradient triple-resonance probe. Spectra were processed using NMRPipe[34] and analyzed using the NMRView[35] software package. The sample was prepared by dissolving ∼2.0 mg of geldanamycin in 0.5 mL of $CDCl_3$ (Aldrich). ^{1}H and ^{1}H−^{13}C 2D spectra (DQF-COSY, HOHAHA, ROESY, HMQC) were accumulated at 298 K.

A gradient-enhanced double-quantum-filtered homonuclear COSY[36] was performed to measure $^3J_{HH}$ coupling constants. ROEs were assigned from a series of ROESY experiments[37] recorded with mixing times of 80, 160, 240, and 320 ms and were quantified by the analysis of the buildup curve of the assigned signals. All the 2D collected spectra were acquired using 4096 per 512 points, setting the spectral width to 12.4 ppm for the indirectly detected dimension and to 15 ppm for the acquisition dimension with the carrier positioned at 6.2 ppm. See Table 1.

Radicicol NMR Data. The ^{1}H resonances of radicicol (25 mM $CDCl_3$) were acquired on a Bruker Avance 400 MHz spectrometer at 298 K and referenced against the solvent signal. The NMR protocol described above for geldanamycin was followed without modification. See Table 2.

Monte Carlo Conformational Searching with MacroModel: Force Fields and NAMFIS Essentials. Coordinates for geldanamycin were obtained from the Cambridge Crystallographic Database.[1] Modification of the solid-state structure[28] was required to generate the protein-bound analogue, namely, replacement of an azetine ring at C-17 by a methoxy group. Structural changes at this position show a negligible effect on the binding conformation, although substitution here often increases the ligand solubility properties.[28] The resulting structure for **1** was used as a starting point for all conformational searches. Three different force fields (AMBER*, MM3*, and MMFFs)[38−42] were used to generate conformations in MacroModel 7.1[43] with the GBSA/$CHCl_3$ solvent model.[44]

Since compound **1** prefers a *trans*-arrangement in the unliganded solid-state structure[28] while displaying a *cis*-conformation in the protein-bound system,[27,28,45] the two amide configurations were utilized separately as starting points for the conformational searches. For each geometry, three force fields were employed to generate possible solution conformations. Each force field search was performed with three 50000-step MCMM (Monte Carlo multiple minimum)[46] runs initiated with a random starting point. The resulting conformers were optimized to

Table 1. ROESY-Derived Distances and Coupling Constants for Geldanamycin in $CDCl_3$

		$^3J_{HH}$ (Hz)			
H3	H4	11.2	H10	H11	<2
H4	H5	11.2	H11	H12	8.5
H9	H10	9.4	H12	H13a,b	6.0
H6	H5	9.4	H14	H15a	9.7
H6	H7	<1.5	H14	H15b	3.2
		ROE-Derived Distances[a] (Å)			
NH	H3	2.3	H9	10-CH_3	3.6
H3	H5	2.8	H7	H6	2.4
H3	H6	2.1	6-OCH_3	H6	2.9
H3	H7	2.9	H10	H11	2.6
H3	6-OCH_3	4.0	H11	10-CH_3	3.6
H4	2-CH_3	2.9	H11	H14	2.2
H5	H7	2.7	H12	H10	2.9
H5	6-OCH_3	3.2	H12	H14	2.8
H9	H7	2.2	H10	8-CH_3	2.8
H9	H11	2.7			

[a] From ROESY buildup curves.

Table 2. ROESY-Derived Distances and Coupling Constants for Radicicol in $CDCl_3$

		$^3J_{HH}$ (Hz)			
H17	H18	6.8	H15	H16b	9.1
H16a	H17	3.3	H14	H15	2.6
H16b	H17	3.6	H13	H14	2.3
H15	H16a	2.6			
		ROE-Derived Distances[a] (Å)			
H18	H16a	2.8	H14	H11	3.3
H18	H15	2.9	H15	H11	4.0
H16a	H17	2.8	H17	H14	3.7
H16b	H17	2.8	H18	H11	3.5
H16b	H14	3.1			

[a] From ROESY buildup curves.

(30) (a) Fesik, S. W.; Gampe, R. T., Jr.; Holzman, T. F.; Egan, D. A.; Edalji, R.; Luly, J. R.; Simmer, R.; Helfrich, R.; Kishore, V.; Rich, D. H. *Science* **1990**, *250*, 1406−1409. (b) Fesik, S. W.; et al. *Biochemistry* **1991**, *30*, 6574−6583.
(31) Loosli, H. R.; Kessler, H.; Oschkinat, H.; Weber, H.-P.; Petcher, T. J.; Widmer, T. J. *Helv. Chim. Acta* **1985**, *68*, 682−704.
(32) Lautz, J.; Kessler, H.; Kaptein, R.; van Gunsteren, W. F. *J. Comput.-Aided Mol. Des.* **1987**, *1*, 219−241.
(33) *GLIDE*, version 4.0; Schrödinger, LLC: New York, 2005.
(34) Delaglio, F.; Grzesiek, S.; Vuister, G. W.; Zhu, G.; Pfiezfer, J.; Bax, A. *J. Biomol. NMR* **1995**, *6*, 277−293.
(35) Johnson, B.; Blevins, R. A. *J. Biomol. NMR* **1994**, *4*, 603−614.
(36) Ancian, B. B.; Dauphin, J. F.; Shaw, A. A. *J. Magn. Reson.* **1997**, *125*, 348−354.
(37) Bax, A.; Davis, D. G. *J. Magn. Reson.* **1985**, *63*, 207−213.
(38) Allinger, N. L.; Yuh, Y. H.; Li, J. H. *J. Am. Chem. Soc.* **1989**, *63*, 8551−8566.
(39) Weiner, S. J.; Kollman, P. A.; Case, D. A.; Singh, U. S.; Ghio, C.; Alagon, G.; Profeta, S.; Weiner, P. *J. Am. Chem. Soc.* **1984**, *106*, 765−784.
(40) Weiner, S. J.; Kollman, P. A.; Nguyen, D. T.; Case, D. A. *J. Comput. Chem.* **1986**, *7*, 230−252.
(41) Halgren, T. A.; Nachbar, R. B. *J. Comput. Chem.* **1996**, *17*, 587−615.
(42) Halgren, T. A. *J. Comput. Chem.* **1999**, *20*, 730−748.
(43) Mohamadi, F. R.; Richards, N. G. J.; Guida, W. C.; Liskamp, R.; Lipton, M.; Caufield, C.; Chang, G.; Hendrickson, T.; Still, W. C. *J. Comput. Chem.* **1990**, *11*, 440−467.
(44) Still, W. C. T.; Tempczyk, A.; Kawley, R. C.; Hendrickson, T. *J. Am. Chem. Soc.* **1990**, *112*, 6127−6129.
(45) Stebbins, C. E.; Russo, A. A.; Schneider, C.; Rosen, N.; Hartl, F. U.; Pavletich, N. P. *Cell* **1997**, *89*, 239−250.
(46) Chang, G.; Guida, W. C.; Still, C. W. *J. Am. Chem. Soc.* **1989**, *111*, 4379−4386.

Table 3. MCMM Conformational Search for *trans*-Geldanamycin (*trans*-**1**)

	AMBER*	MM3*	MMFFs
no. of opt conformers	197	339	183
GE (kJ/mol)	−98.5	177.7	142.8
no. of times GEM found	205	63	166

Table 4. MCMM Conformational Search for *cis*-Geldanamycin (*cis*-**1**)

	AMBER*	MM3*	MMFFs
no. of opt conformers	155	301	71
GE (kJ/mol)	−75.2	171.4	177.9
no. of times GEM found	54	184	407

Table 5. MCMM Conformational Search for Radicicol (**2**)

	AMBER*	MM3*	MMFFs
no. of opt conformers	118	213	51
GE (kJ/mol)	41.0	77.2	187.6
no. of times GEM found	1711	1835	2713

convergence by sequential treatment with the Polak−Ribiere conjugate gradient (PRCG)[47] and truncated Newton conjugate gradient (TNCG)[48] algorithms with a 25 kJ/mol cutoff. The number of times the global energy minimum (GEM) is located for each force field is a measure of the completeness of a conformational search, 10−15 times ordinarily being regarded as sufficient.[46] Tables 3 and 4 provide results for the *trans* (*trans*-**1**) and *cis* (*cis*-**1**) isomers, respectively. In total, 1246 conformations were generated for **1**.

Conformational searches for radicicol (Table 5) were also performed in a $CHCl_3$ continuum model using the methods described for geldanamycin. A total of 382 optimized conformations were generated.

Docking NAMFIS-Selected Conformations into Hsp90. Schrödinger's docking program GLIDE (grid-based ligand docking with energetics) was employed to dock the collection of NAMFIS-derived geldanamycin and radicicol structures into the 1YET[45] and 1BGQ[26] crystal structure Hsp90 pockets, respectively. The protocol is as follows.

(1) All crystallographic waters were deleted.

(2) Protein preparation. Hydrogens and OPLS-defined atomic parameters were assigned to protein residues, and minimization was performed until the RMSD of all heavy atoms was within 0.8 Å of the crystallographically determined positions. Residues were not neutralized.

(3) Grid generation. The crystallographic locus of geldanamycin was used as the center of the grid box. No constraints were employed in the docking.

(4) Ligand docking. Extra-Precision mode was utilized during ligand docking. van der Waals radii were scaled by 0.8 for nonpolar atoms. For multiple ligand docking experiments, an output maximum of 10000 ligand poses per docking run with a limit of 600 poses for each ligand was adopted. All NAMFIS conformations (including those rejected by energy) were submitted for docking.

For geldanamycin, the 12 NAMFIS conformers were GLIDE-docked to generate a total of 52 poses, the highest scored top 10 of which are reported in Table 11. The same protocol was followed for the six radicicol NAMFIS conformers. GLIDE-docking of the latter into the 1BGQ crystal structure delivered a total of 10 unique poses (Table 12).

DFT Enthalpic Calculations of *cis*- and *trans*-Geldanamycin. Previous density functional theory (DFT) quantum chemical calculations by Lee et al. have suggested that *cis*-geldanamycin is an unlikely conformation in solution, since selected structures show a 15.5 kcal/mol enthalpic difference between *cis*- and *trans*-forms favoring the *trans*-form.[49] The same work estimated the isomerization barrier to be in excess of 20 kcal/mol. Suspecting that the 16 kcal/mol energy difference is a serious overestimate, we reevaluated the open and compact rotamers of geldanamycin (Figure 2) with a more extended basis set and a more rigorous solvation model than employed by Lee et al. The calculations were performed in Gaussian03.[50]

Table 6. Relative DFT Energies for the X-ray Structures of Geldanamycin *cis*- and *trans*-Isomers Depicted in Figure 2 (Becke3LYP/6-311+G**//MMFFs and the PCM Solvation Model)

PCM solvent model	*E*(rel),[a] kcal/mol	*cis* population,[b] %	*cis*, au	*trans*, au
water	−2.3	2.0	−1916.198418	−1916.202101
DMSO	−1.9	3.9	−1916.194420	−1916.197389
$CHCl_3$	−3.8	0.2	−1916.185952	−1916.179978
gas	−8.3	0.0	−1916.147638	−1916.160874

[a] *E*(rel) = (*trans* − *cis*) × 627.5 (i.e., 627.5 kcal/au), *trans* being the lowest. [b] Boltzmann distribution, 298 K.

In the present work, the open *trans*-structure was derived from the Cambridge Crystallographic Database, while the compact *cis*-conformer was extracted from the 1YET geldanamycin−Hsp90 complex[45] available in the Protein Databank.[2] Torsionally constrained geometry optimization and energy evaluation for both structures were performed with the Becke3LYP/6-311+G**//MMFFs protocol using the PCM solvation model.[51] It is noteworthy that the previous quantum chemical analysis (Becke3LYP/6-31G*//Becke3LYP/6-31G*) employed the Onsager model[52] to simulate solvent interaction with geldanamycin. This method creates a sphere around the ligand that reflects the molecule's general electrostatic character, the surrounding reaction field interacting with the surface of the sphere. By contrast, the PCM solvation model assigns an individual solvation sphere to each atom in the molecule, thereby yielding a more atomistic and therefore conformationally more sensitive estimate of the molecule's electrostatic character in the context of the surrounding reaction field. The results of applying several PCM solvent models to the optimized *cis*- and *trans*-isomers of Figure 2 are provided in Table 6.

Results and Discussion

Crystal Structure Conformations of 1 and 2. The X-ray crystal structures presented by Roe and co-workers[27] demonstrate that structurally divergent **1** and **2** bind to the same ATP pocket on the Hsp90 protein (Figure 1). Geldanamycin consists of a 19-membered ring with 14 single bonds in the ring responsible for its conformational diversity. In spite of the corresponding theoretical number of different rotational isomers (ca. 3^{14}), the actual number of feasible conformers for the antibiotic is curtailed by the ring, an amide bond, three double bonds, and six functional groups with the potential to participate in hydrogen-bonding (see below). Nonetheless, examination of the solid-state and protein-bound crystal structures for **1** (Figure 2) suggests that considerable conformational reorganization is required for the molecule to transit from the solid state to the bound form.

By contrast, radicicol with 10 rotatable bonds is smaller and less flexible than geldanamycin. The 14-membered ring sustains 2 double bonds and 5 potential H-bonding functional groups for added structural rigidity. The reduced conformational diversity is underscored by the conformational searches for radicicol and geldanamycin, yielding 382 and 1246 conforma-

(47) Polak, E.; Ribiere, G. *Rev. Fr. Inf. Rech. Oper., Ser. Rouge* **1969**, *16*, 35.
(48) Ponder. J. W.; Richards, F. M. *J. Comput. Chem.* **1987**, *8*, 1016−1024.
(49) Lee, Y.-S.; Marcu, M. G.; Neckers, L. *Chem. Biol.* **2004**, *11*, 991−998.
(50) Frisch, M. J.; et al. *Gaussian 03*, revision C.02; Gaussian, Inc.: Wallingford, CT, 2004.
(51) Miertus, S.; Tomasi, J. *Chem. Phys.* **1982**, *65*, 239−245.
(52) Onsager, L. *J. Am. Chem. Soc.* **1938**, *58*, 1486−1493.

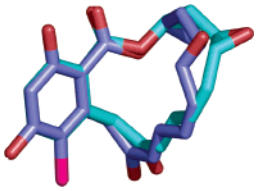

Figure 3. Solid-state structure of radicicol (blue) overlapped with its protein-bound conformation (cyan). Unlike geldanamycin, the two structures of radicicol superimpose almost perfectly. All functional groups are positioned in approximately the same location.

Table 7. Geldanamycin Conformer Populations (NAMFIS) and Relative Free Energies, 298 K[a]

conformer	population, %	ΔG(rel),[b] kcal/mol	conformer	population, %	ΔG(rel),[b] kcal/mol
1	**22**	**0.0**	**7**	**4**	**1.0**
2	17	0.2	8	4	1.0
3	16	0.2	**9**	**4**	**1.0**
4	12	0.4	10	4	1.0
5	7	0.7	11	3	1.2
6	7	0.7	12	2	1.4

[a] *cis*-Conformations are highlighted in bold. [b] Boltzmann distribution calculated at 298 K.

tions, respectively, under the same computational conditions. A comparison of solid-state and protein-bound forms (Figure 3) might suggest that, unlike geldanamycin (Figure 2), radicicol involves significantly less conformational reorganization as the free form is converted to the bound conformation. However, such a comparison fails to take into account the conformational profiles of the two molecules in solution. This point is discussed below.

Solution Conformations of 1 and 2 from NAMFIS Deconvolution. Estimation of the solution conformations for **1** and **2** in the present work has required a combination of NMR and computational experiments. 2D ROESY NMR in $CDCl_3$ was performed to provide 19 ROE distances and 10 three-bond coupling constants ($^3J_{HH}$) for geldanamycin (Table 1) and 9 ROE distances and 6 $^3J_{HH}$ values for radicicol (Table 2). Extensive Monte Carlo conformational searches for both molecules were carried out using MM3*, AMBER*, and MMFFs force fields. The fully optimized structures were relieved of duplicates, loaded into a common structural database, and subjected to a NAMFIS conformational deconvolution using the NMR-averaged interatomic distances and torsion angles. This treatment, which intersects computed and NMR-determined geometries, resulted in 12 geldanamycin conformations with estimated populations ranging from 2% to 22% and 6 radicicol conformers with populations from 7% to 25%. Additional post-NAMFIS evaluations of the conformers were performed to ensure that they are both chemically reasonable and characterized by low energy.

For geldanamycin, approximately 70% of the NAMFIS-derived structures prefer the *trans*-amide conformation, while 30% exhibit the *cis*-arrangement. Interestingly, analysis of the NAMFIS results suggests the most populated conformer (22%, Table 7) to be a *cis*-amide. This is in qualitative agreement with the assessment that *cis*- and *trans*-amide isomers of geldanamycin are separated by small energy gaps that are most likely solvent dependent (Tables 6, 7, and 9). In Figure 4a, the most stable *cis*-form differs significantly from the bound *cis*-form (Figure 4d). As discussed below, however, the individual

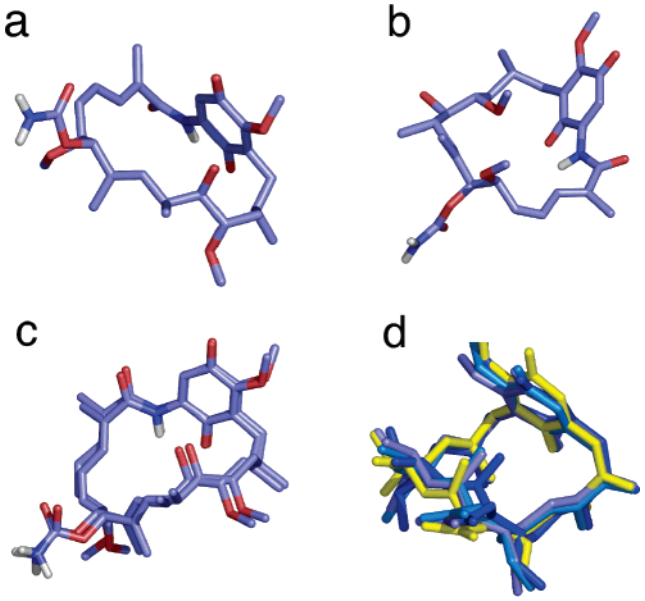

Figure 4. NAMFIS and crystal structure conformations of geldanamycin: (a) *cis*-NAMFIS-1; (b) *trans*-NAMFIS-2; (c) *trans*-NAMFIS-3 and the "free" solid-state conformer; (d) overlap of geldanamycin and 17-DMG in 1A4H (marine blue), 1OSF (blue), and 1YET (slate) with *cis*-NAMFIS-9 in yellow.

Table 8. Radicicol Conformer Populations (NAMFIS) and Relative Free Energies, 298 K

conformer	population, %	ΔG(rel),[a] kcal/mol	conformer	population, %	ΔG(rel),[a] kcal/mol
1	25	0.0	4	17	0.2
2	21	0.4	5	12	0.4
3	18	0.2	6	7	0.7

[a] Boltzmann distribution calculated at 298 K.

population values of *cis* solution conformers should be taken only as an approximation. Among the NAMFIS-derived conformations, *trans*-NAMFIS-3 (16%) mimics the unbound crystal structure geometry determined by Schnur and Corman.[36] Heavy atom overlap of the two forms (Figure 4c) yields a diminutive RMSD of 0.42 Å. *Cis*-NAMFIS-9 (4%) confirms that the bound form is likewise represented as a contributor to the solution average. Except for the spatial orientations of the two methoxy groups at C-6 and C-17, it is virtually superimposable with Roe et al.'s protein-bound conformation (heavy atom RMSD = 0.8 Å, Figure 4d). Table 7 also records the Boltzmann free energies associated with the populations assumed to be at 298 K. Relative DFT energies including PCM solvation were obtained using the treatment described earlier (Becke3LYP/6−311+G**//MMFFs) (Table 9).

With respect to conformational reorganization in **1**, since the ^{1}H NMR spectrum is a well-resolved average, 12 conformations are presumed to participate in an equilibrium that is rapidly established well below room temperature. Thus, binding to Hsp90 could involve direct capture of the solution version of the bound form (conformer 9, Table 7). Alternatively, the more populated *cis*-and *trans*-conformers (22% and 17%, respectively) might be weakly complexed to the protein followed by a low-energy induced fit. In either case, depletion of the conformational pool is accompanied by immediate redistribution of torsional forms by virtue of an equilibrium shift.

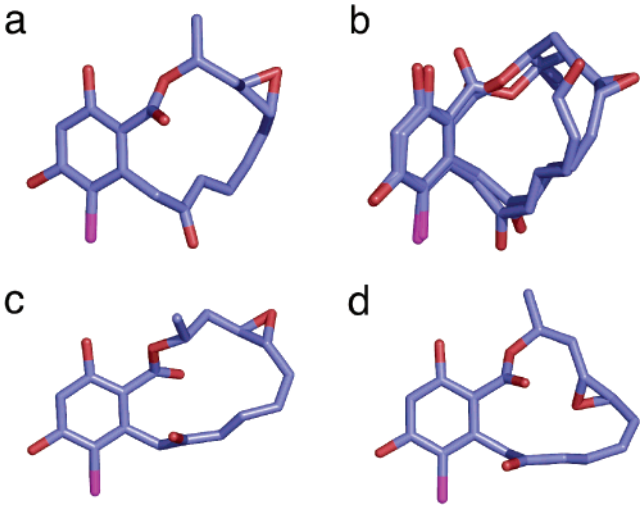

Figure 5. NAMFIS (Table 8) and crystal structure conformations of radicicol: (a) NAMFIS-1; (b) NAMFIS-2 and the solid-state conformer; (c) NAMFIS-3; (d) NAMFIS-4.

For radicicol, NAMFIS selected six conformations with populations ranging from 7% to 25% (Table 8). The top four conformers are depicted in Figure 5. Significantly, the second-ranked form (21%, Figure 5b) matches the protein-bound and the solid-state forms pictured in Figure 2 (RMSD = 0.6 Å vs the solid-state structure). The congruence of the solid-state and protein-bound conformer structures has led to the argument that radicicol pays less of an entropic penalty during the binding event to Hsp90 by comparison with geldanamycin.[27] As described by Roe et al.,[27] **1** binds with a favorable enthalpy ($\Delta H^{298} = -10.0$ kcal/mol) but unfavorable entropy ($T\Delta S^{298} = -1.9$ kcal/mol) at 298 K, leading to micromolar affinity ($K_d = 1.2$ μM, $\Delta G^{298} = -8.1$ kcal/mol). By contrast, radicicol's 64-fold greater binding is entropy driven ($\Delta H = -8.1$ kcal/mol, $T\Delta S^{298} = +2.5$ kcal/mol), resulting in nanomolar affinity ($K_d = 19$ nM, $\Delta G^{298} = -10.5$ kcal/mol).

A somewhat different interpretation of the entropy-dominated binding of radicicol to Hsp90 flows from the NAMFIS analysis. In contrast to the static picture implied by the superposition of solid-state and protein-bound radicicol conformers (Figure 3), the favorable $T\Delta S$ can be seen as a consequence of solution dynamics. There are 12 geldanamycin conformers available for interaction with the protein. The bound form, *cis*-NAMFIS-9, is estimated to exist with a mole fraction of only 0.04 (4%, Table 7). Either the highly unlikely event of productive collision of the latter with Hsp90 or extensive conformational reorganization, or both, contributes to the −1.9 kcal/mol $T\Delta S$ component. Radicicol, similar to geldanamycin, does not present the bound conformation as the highest populated form in solution. However, the second most populated (NAMFIS-2, mole fraction 0.21, 21%) is a close mimic of the bioactive form. Furthermore, only half as many conformers participate in equilibrium conformational reshaping by comparison to geldanamycin. Both of these factors are undoubtedly important elements for the observed +2.5 $T\Delta S$.

Post-NAMFIS Evaluation. NAMFIS accepts and rejects conformations on the basis of geometric data alone without regard for chemical reasonability. While all conformations are fully optimized with one of the force fields employed, an energy acceptance window that is too large in the context of a given problem can lead to the selection of poor-quality structures as a contributor to the NMR average. The energy window for the geldanamycin and radicicol conformational searches was set at 6 kcal/mol above the global minimum. This is a compromise that experience suggests is capable of limiting the number of chemically unreasonable structures in the dataset while allowing viable structures to be considered. In addition to imposing this conservative energy window, however, we have performed a post-NAMFIS evaluation to determine whether the NAMFIS conformations contain anomalous features that identify them as high-energy structures. In particular, steric conflicts such as hydrogen−hydrogen contacts and *syn*-pentane interactions were sought as signatures of poor structures.[16] A scan for intermolecular hydrogen bonding was also executed.[16] H-bonds add stabilizing features that counteract destabilizing steric effects and thereby reinforce a conformation's likelihood to exist in solution. Summaries of the number of these interactions for each conformer are provided in the Supporting Information (Tables S2 and S3). Conformations with exceedingly high relative energies using different solvent models (Tables 9 and 10) were rejected, i.e., geldanamycin conformations 7, 10, and 11 and radicicol conformations 3 and 4. In both ensembles, the bioactive conformations survived.

The energy differences between geldanamycin conformers 5 and 10 were reevaluated to determine the source of the high energies. Geometries were reoptimized without torsional constraints using both OPLS2005[53] and B3LYP/6-31G*. RMS differences relative to the corresponding Table 9 structures are 0.22−0.55 Å, respectively. Thus, the conformations are faithfully reproduced with no apparent changes in geometries upon visual inspection or superposition. Single-point energies for the

Table 9. Relative Energies (kcal/mol) of NAMFIS-Selected Geldanamycin Conformations Treated by Various PCM-Based Solvent Models (Becke3LYP/6-311+G**//MMFFs)

	ΔE(rel)		
conformation	gas	DMSO	H_2O
1	6.7	5.7	4.4
2	7.2	4.6	4.2
3	3.7	3.5	2.9
4	4.1	6.7	7.4
5	0.0	0.0	0.0
6	3.8	2.3	1.9
7	15.8	13.9	14.9
8	5.0	2.7	2.5
9	7.2	4.6	6.2
10	24.6	25.2	24.8
11	16.2	17.2	18.4
12	5.0	6.1	6.8

Table 10. Relative Energies (kcal/mol) of NAMFIS-Selected Radicicol Conformations Treated by Various PCM-Based Solvent Models (Becke3LYP/6-311+G**//MMFFs)

	ΔE(rel)		
conformation	gas	DMSO	H_2O
1	0.0	3.1	3.3
2	3.9	0.0	0.0
3	6.6	10.3	10.5
4	6.2	8.2	8.5
5	3.3	5.2	3.3
6	1.6	5.0	1.6

(53) Kaminski, G. A.; Friesner, R. A.; Tirado-Rives, J.; Jorgensen, W. J. J. *J. Phys. Chem. B* **2001**, *105*, 6474−6487.

Table 11. Scoring Results for GLIDE Docking of Geldanamycin NAMFIS Conformers into Hsp90 (1YET) (kcal/mol)[a]

conformer	GScore[b]	EModel[b]	energy[b]	RMSD[c] (Å)	prime MM-GBSA
NAMFIS-5	−6.3	−39.6	−31.5	7.0	−16.5
NAMFIS-2	−6.0	−49.7	−36.4	8.2	−16.3
NAMFIS-6	−5.8	−50.5	−38.0	6.4	−3.2
NAMFIS-6	−5.8	−55.4	−41.6	6.4	−4.9
NAMFIS-6	−5.7	−54.4	−41.7	6.4	−6.4
NAMFIS-12	−5.7	−45.0	−32.1	8.0	−4.3
NAMFIS-9	**−5.7**	**−55.3**	**−39.7**	**1.2**	**−48.7**
NAMFIS-7	−5.6	−49.4	−39.9	3.6	−16.2
NAMFIS-12	−5.6	−48.8	−36.9	8.0	−7.5
NAMFIS-7	−5.5	−51.2	−36.9	4.5	−12.0

[a] Bioactive (crystallographic) conformation highlighted in bold. [b] Scoring functions employed by the GLIDE procedure. [c] Versus the geldanamycin position in the X-ray crystal structure (1YET).

Table 12. Scoring Results for GLIDE Docking of Radicicol NAMFIS Conformers into Hsp90 (1BGQ) (kcal/mol)[a]

conformer	GScore[b]	EModel[b]	energy[b]	RMSD[c] (Å)	primeMM-GBSA
NAMFIS-1	−7.5	−53.7	−39.9	4.9	−19.4
NAMFIS-3	−7.2	−44.7	−31.8	5.7	−25.9
NAMFIS-3	−7.1	−44.0	−30.9	5.8	−28.2
NAMFIS-3	−7.0	−49.9	−37.3	5.7	−28.1
NAMFIS-2	**−6.8**	**−49.9**	**−36.7**	**1.6**	**−47.6**
NAMFIS-1	−6.5	−55.5	−41.4	5.5	−22.7
NAMFIS-4	−4.6	−41.0	−28.0	5.6	−20.2
NAMFIS-4	−4.6	−42.9	−31.2	5.8	−25.1
NAMFIS-4	−4.4	−44.0	−32.9	5.2	−15.7
NAMFIS-4	−4.3	−45.5	−34.0	5.8	−25.4

[a] Bioactive (crystallographic) conformation highlighted in bold. [b] Scoring functions employed by the GLIDE procedure. [c] Versus the radicicol position in the X-ray crystal structure (1BGQ).

latter structures were reevaluated with B3LYP/6-311+G**, resulting in energy differences of 4.9 and 3.3 kcal/mol, respectively. As a result, although no significant structural changes were observed by alternative optimization, the energies were reduced by ~20 kcal/mol. This suggests that the MMFFs parametrization has introduced subtle components of strain that are avoided by DFT and newer force fields such as OPLS2005.

Despite the population analysis and post-NAMFIS evaluation of it described above, it should be recognized that the absolute NAMFIS population of the highest ranked *cis*-amide conformer (**1**, 22%) is in contrast with the NMR experiment. Assuming a normal amide rotation barrier (16−21 kcal/mol),[54] a 2−22% population of the *cis*-form should be readily detected in the room-temperature NMR spectrum. In fact, it is identified by neither the 1D nor the ROESY spectra. As mentioned above, the populations of polar substances such as geldanamcin are expected to be solvent dependent. The PCM calculations of Table 6 suggest that the energy gap between the *trans*- and *cis*-conformers sampled increases as the polarity of the medium decreases. In $CDCl_3$, the solvent employed in the present study, the population estimated at <1% suggests the concentration of the *cis*-form to be so low that it is undetectable by NMR. Whatever the amount of *cis*-conformer in solution, the calculations concur that the *trans*-isomer remains heavily dominant in all solvents.

Why might the NAMFIS treatment overestimate the contribution of the *cis*-isomer? There are a variety of error points in analyses such as NAMFIS that derive from both the actual measurement and the parametrization quality of the accompanying force fields. Such errors have been discussed by Cicero and colleagues in the seminal NAMFIS paper.[3] More recently, in an application of the method to laulimalide, we reported an error analysis which demonstrated that the populations of individual conformations in some cases can be highly variable in response to experimental errors.[16] Importantly, however, while such errors may lead to significant population reranking of individual conformers, family identity is retained. We ascribe the origin of the high NAMFIS population of *cis*-geldanamycin to this source. Nonetheless, the weight of the evidence supports the presence of both *trans*- and *cis*-conformational families, the *cis*-form falling at the edge of or under the NMR horizon.

NAMFIS-Selected Conformers as Bioactive Candidates: Protein Docking. The original intent of the present work was to determine whether the bioactive conformations of molecules that block Hsp90 are found both in solution and within the protein ATP binding pocket. A related question concerns the possibility of predicting ligand-binding poses without taking advantage of prior knowledge of the Hsp90−ligand complex structures. The proliferation and evaluation of docking programs suggest this to be an achievable goal.[55,56] Most docking procedures are able to explore the conformations of acyclic candidate ligands as part of the docking exercise, but are generally unable to accomplish this task for complex cyclic structures such as **1** and **2**. In such cases, one is obligated to perform a priori a complete conformational search of the cyclic core followed by docking of each ring conformation supplemented by an on-the-fly conformational search of any substitutents or side chains. As a potential alternative, we asked whether a well-tested docking algorithm, namely, GLIDE, could employ *only* the NAMFIS solution conformations to generate ligand poses similar to those found in crystal structures.

As a preliminary, we note that two X-ray crystal structures of geldanamycin and the 17-DMAG analogue bound to Hsp90 (1A4H,[27,57] 1YET,[45] and 1OSF,[28] respectively) reveal a common *cis*-amide conformation. Of the nine acceptable solution conformations of **1** identified by NAMFIS, only one (*cis*-conformer 9, 4% population, Table 7) shows ring torsional properties similar to those of the Hsp90-bound ligands found in the crystal lattice. Figure 4d displays a heavy atom superposition of the four bound forms and conformer 9 (*cis*-NAMFIS-9, yellow). An Extra-Precision GLIDE docking study of geldanamycin predicts the latter (the most bioactive-like of the NAMFIS series) to be within the top 10 of 52 binding poses with an RMSD of 1.2 Å relative to the 1YET crystallographic pose (Table 11). In the same way, radicicol's NAMFIS-2 (most similar to the bioactive crystal structure of 1BGQ) was ranked within the 10 total binding poses (Table 12). The fact that neither bioactive pose was ranked as the top pose makes this analysis less than ideal in the context of a purely predictive versus retrospective study. Since the interaction of both ligands with the protein is mediated in part by water molecules, we reasoned that incorporation of a water model into the docking procedure might

(54) Eliel, E. L.; Wilen, S. H. *Stereochemistry of Organic Compounds*; John Wiley & Sons, Inc.: New York, 1994; pp 553−554.

(55) Wang, R.; Lu, Y.; Fang, X.; Wang, S. *J. Chem. Inf. Comput. Sci.* **2004**, *44*, 2114−2125.

(56) Warren, G. L.; Andrews, C. Webster; Capelli, A.-M.; Clarke, B.; LaLonde, J.; Lambert, M. H.; Linvall, M.; Nevins, N.; Semus, S. F.; Senger, S.; Tedesco, G.; Wall, I. D.; Woolven, J. M.; Peishoff, C. E.; Head, M. S. *J. Med. Chem.* **2006**, *49*, 5912−5931.

(57) Prodromou, C.; Roe, M. S.; O'Brien, R.; Ladbury, J. E.; Piper, P. W.; Pearl, L. H. *Cell* **1997**, *90*, 65−75.

improve the ranking of the GLIDE poses with respect to the known bioactive conformations. Accordingly, MM-GBSA calculations[58] were performed postdocking.

Free energy perturbation calculations are often used to determine the binding free energy of a ligand to a protein by means of molecular dynamics simulations in an explicit water environment. While the procedure can accurately deliver both absolute and relative free energies in favorable cases, the calculations are exceptionally resource-expensive when a docked list of conformations is evaluated against a target receptor. By contrast, the MM-GBSA method combines molecular mechanics calculations and a continuum solvent treatment to estimate the ligand-binding affinity. Although not accurate in absolute energy terms, the calculations can be used as an independent scoring system for ranking docked structures. In the present case, MM-GBSA was performed by applying Schrödinger's Prime MM-GBSA script[57c] to the 52 and 10 GLIDE docking poses for geldanamycin and radicicol, respectively. Of the top 10 geldanamycin poses, NAMFIS-9 unambiguously achieves the top MM-GBSA score. Similarly, radicicol's NAMFIS-2 conformer is the clear-cut top MM-GBSA scorer among the 10 GLIDE poses. These results underscore the utility of employing NAMFIS conformers as protein-docking candidates in tandem with an accurate scoring function in the search for experimentally viable protein-bound conformations.

Summary and Conclusions

In the present work we seek to evaluate the capacity of solution conformational profiles of small druglike molecules for predicting the corresponding protein-bound conformations under circumstances where crystallographic resolution is low or when homology models are used as protein surrogate structures. We chose **1** and **2** as test cases, since X-ray crystal structures of both molecules in the Hsp90 protein and in a "free" solid-state form are known. In addition, although the compounds are both blockers of Hsp90's actions, they operate with significantly different efficacies, namely, at micromolar versus nanomolar concentrations, respectively. Furthermore, the compounds are of sufficiently different molecular weight, ring size, and functionality that standard pharmacophoric comparisons are not straightforward. Figure 1 depicts their experimental binding poses in Hsp90. As a consequence, analysis of the conformation across solution, crystalline, and protein-bound states offers a unique opportunity to uncover the connections among the different environments and to learn whether observations in solution can be carried over as a predictive tool for protein binding.

For the solution state, we employed NAMFIS methodology to identify collections of equilibrating conformations derived by deconvoluting the averaged NMR spectra of **1** and **2**. An important benefit of this treatment is the derivation of an estimated population of the individual conformations. We have shown previously that the method leads to uncertainties in identification of individual conformers, but that family types are faithfully reproduced.[15,16] In the present case, both the 6- and 12-membered conformer pools of radicicol and geldanamycin, respectively, contain the solid-state conformations in addition to the protein-bound forms as equilibrium contributors below a mole fraction of 0.25 (geldanamycin, 4%; radicicol, 21%). The higher population for radicicol may be attributed to the fact that its core ring is smaller and characterized by a relatively reduced conformational mobility.

Not only do we find the X-ray crystallographic poses among the NAMFIS-determined solution conformations for geldanamycin and radicicol, but we have also reverse-engineered the structural problem by employing these conformations as docking candidates for predicting the experimental binding poses in the unliganded proteins. With the GLIDE docking procedure and its associated scoring functions, the experimental conformers and poses are found among the top 10 ranked complexes. However, by reevaluating the energies of the latter with the MM-GBSA procedure, the experimental structures are unambiguously identified as the favored solution (Tables 11 and 12). This result should be tempered by the fact that ligands were redocked into their native proteins and unaccompanied by cross-docking studies.

We anticipate that the work reported here will aid in the determination of the ligand conformation for protein complexes at low resolution or in the absence of an explicit X-ray crystal structure of the specific complex under study.

Acknowledgment. This work was financially supported in part by the National Institutes of Health (Grant 1 U54 HG003918-01). We are grateful to Professor Dennis Liotta (Emory University) for encouragement of the study.

Supporting Information Available: Summaries of the number of interactions for each conformer and complete refs 25, 30b, and 50. This material is available free of charge via the Internet at http://pubs.acs.org.

JA064863P

(58) (a) http://www.scfbio-iitd.res.in/doc/MMGBSA.pdf. (b) http://www.accelrys.com/accelrysworld/posters/cb28_deepak_singh.pdf. (c) https://www.psgvb.com/Download.php?mID=8&sID=50&cID=10004.